Solvation Structure of Uracil in Ionic Liquids

Norman, S. E., Turner, A. H., Holbrey, J. D., & Youngs, T. G. A. (2016). Solvation Structure of Uracil in Ionic Liquids. ChemPhysChem, 17(23), 3923-3931. DOI: 10.1002/cphc.201600984

Published in:
ChemPhysChem

Document Version:
Peer reviewed version

Final accepted draft for ChemPhysChem, doi:10.102/cphc.201600984

Solvation Structure of Uracil in Ionic Liquids

Sarah E. Norman,[a,b] Adam H. Turner,[b] John D. Holbrey,[b] and Tristan G. A. Youngs*[a]

Abstract: The local solvation environment of uracil dissolved in the ionic liquid 1-ethyl-3-methylimidazolium acetate has been studied using neutron diffraction techniques. At solvent:solute ratios of 3:1 and 2:1 ionic liquid:uracil, little perturbation of the ion-ion correlations compared to those of the neat ionic liquid are observed. We find that solvation of the uracil is driven predominantly by the acetate anion of the solvent. While short distance correlations exist between uracil and the imidazolium cation, the geometry of these contacts suggest that they cannot be considered as hydrogen bonds, in contrast to other studies by Araújo et al. (J. M. Araújo, A. B. Pereiro, J. N. Canongia-Lopes, L. P. Rebelo, I. M. Marrucho, *J. Phys. Chem. B* **2013**, *117*, 4109-4120). Nevertheless, this combination of interactions of the solute with both the cation and anion components of the solvents helps explain the high solubility of the nucleobase in this media. In addition, favorable uracil-uracil contacts are observed, of similar magnitude to those between cation and uracil, and are also likely to aid dissolution.

Introduction

Mainstream interest in using ionic liquids (ILs) as solvents has grown enormously over the past twenty years.[1] However, in comparison to developments of synthetic chemistry and materials applications,[2] the reactions and key solvation processes responsible for chemical transformations in ILs are less clearly understood.[3] Until such time as this crucial information on both general and specific ion-ion and ion-solution interactions can be defined and incorporated into new models for solvation,[4] critical systems have to be studied on a case-by-case basis.

One area of particular interest to us to understand the function of ILs as solvents for biomaterials.[5] Following the first report on the dissolution of cellulose in 1,3-dialkylimidazolium halide ILs,[6] a number of families of ILs with basic, hydrogen-bond accepting anions including acetate ($[OAc]^-$) and dimethylphosphate ($[R_2PO_3]^-$)[7] have positively been identified as cellulosic solvents. Moreover, it has been shown that these ILs can be diluted, using dipolar aprotic diluents such as, 3-dimethyl-2-imidazolidinone, dimethylsulfoxide, and sulfolane, and still retain the solubilising power.[8] Mao *et al.* have recently assigning the ability of these ILs to function as strongly dissociating solvents to an '*ionic liquid effect*' based on measurement of the absolute pK_as values for weakly polar aprotic ILs.[9] Dissolution and functionalisation of many simple sugars, cyclodextrins, cellulose, starch, and chitin/chitosan biopolymers have also been studied,[10] as have a number of other hydrogen-bonded biomolecular systems (DNA,[11] peptides,[12] and nucleosides[13] *etc*).

In order to better understand the properties of ILs, and specifically the interactions present that lead to the high solubilities of these biomaterials in ILs such as 1-ethyl-3-methylimidazolium acetate, molecular dynamics,[14] NMR,[15] neutron[5,16] and x-ray diffraction[17] studies have been conducted. Of these approaches, neutron diffraction is amongst the most powerful since, in principle, results obtained contain a detailed description of the correlations in the system under study (depending, of course, on the capabilities of the instrument employed). Moreover, isotopic substitution of some elements enables the relative weights of the partial structure factors of the system to be altered by changing the isotopic composition of the samples. Such substitutions affect the resulting total structure factor but without, in principle, affecting the chemical properties of the system. Of all elements, the most useful isotopic substitution from a chemical perspective is that of changing ubiquitous hydrogens to deuterium (^{2}H), since the coherent scattering properties of the two isotopes differ significantly. This provides multiple spectral data sets on structurally 'identical' systems with which to fit simulation models (the approach used in the present study).

Strong solute-anion interactions are generally considered to be the driving force behind structure and solvation of polar or hydrogen-bonding solutes in ILs. The role of the cation is often regarded as secondary to that of the anion, especially when the cation is a relatively weak interactor. For ILs with the archetypal 1,3-dialkylimidazolium cation, the aromatic hydrogen sites on the imidazolium ring are of most interest with the C2 position having the greatest acidity. This is usually manifest through cation-anion hydrogen-bonding motifs in neat ILs (identified by IR and NMR spectroscopy)[18] and in the solid state (from X-ray crystallography).[19]

Interactions (and indeed reactions) at the C2 position can be important, as for example in the formation of imidazolium-2-carboxylate zwitterions (*masked carbenes*).[20] However for the dissolution of simple monomeric and oligomeric sugars (cyclodextrins, cellulose, starches *etc*), formation of strong hydrogen-bonds between sugar-hydroxyl groups as hydrogen-bond donors and the solvent anions as hydrogen-bond acceptors is the dominant mechanism.[5c]

[a] Dr S. E. Norman, Dr T. G. A. Youngs
ISIS Facility
STFC Rutherford Appleton Laboratory
Harwell Campus, Didcot, Oxfordshire, OX11 0QX
E-mail: tristan.youngs@stfc.ac.uk
[b] A. H. Turner, Dr J. D. Holbrey
School of Chemistry and Chemical Engineering
David Keir Building
Queen's University Belfast
Belfast, Northern Ireland, BT9 5AG

Supporting information for this article is given via a link at the end of the document.

Araújo et al. have recently used ^{13}C and ^{1}H and 2D NOESY NMR spectroscopy combined with QM calculations to study the solvation of uracil and other nucleobases in 1-ethyl-3-methylimidazolium acetate ([EMIM][OAc]).[21, 22] Hydrogen bonding interactions between uracil amine hydrogens and oxygen atoms of the IL acetate anions were identified. In addition, significant hydrogen bonding between the cation hydrogen at the C2 position of the imidazolium ring and the carbonyl groups of the nucleobases was described, most notably with uracil. Both nucleobase hydrogen-bond donating and accepting sites play vital roles in the encoding and transmission of information through base-pairing in DNA and RNA. Consequently, the observation that both the cation and anion of the IL solvent have key contributions to the solvation of nucleobases is both expected and notably different to cases with carbohydrates and sugars and builds an elegant picture of the dissolution mechanism of nucleobases, requiring co-operative solvation by both ions of the ionic liquid. In order to understand, for instance, the structure and solvation of biomolecules in solvated in ionic liquids (a growing area of research owing to the stabilising properties of the IL),[23] a practical starting point is the individual nucleic acid bases, for which the precise solvation details can be more easily extracted.

Here we apply total neutron scattering with isotopic substitution to the study of two different concentrations of uracil in the ionic liquid [EMIM][OAc], in order to more fully characterise the liquid structure present in these systems. Measurements on the neat IL were also made, and structural changes described in the context of this reference system. All presented quantities for the neat IL and mixtures are derived from the simulations of the measured data in the present study (see Experimental section for details).

Results and Discussion

Atom numbering and isotopic substitutions for each component are shown in Figure 1, while experimental F(Q) along with simulated data for all uracil-containing systems are shown in Figure 2. Data for the neat IL is presented in the supplementary information (Figure SI.1), and is consistent with that previously reported.[5d] For all datasets, good agreement between the EPSR simulation and measured neutron scattering patterns is observed.

Figure 3 shows the centre of mass radial distribution functions (RDFs) between the IL cation and anion components and the solute for the pure IL and uracil-containing systems. We note the

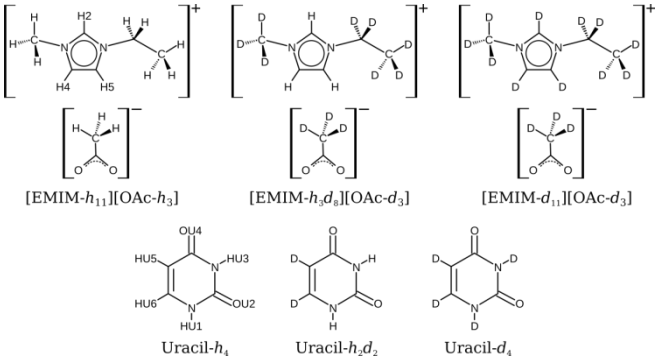

Figure 1. Atom numbering and isotopic substitutions of [EMIM][OAc] and uracil.

anticipated strong correlation between cation and anion, negligible correlations between cations, and modest correlations between anions consistent with previous measurements. These correlations give rise to the features at 4.5 and 8.0 Å which correspond to anion association (clustering via methyl groups) and correlations between anions bound to the same cation respectively. On the addition of uracil to the system, the ion-ion correlations between remain largely unaffected, indicating that the system is able to solubilise the nucleobase without sacrificing the interactions which characterise the bulk liquid. At the higher uracil concentration, a slight shift of some intensity in the cation-anion peak to shorter *r* is observed, and the second peak in the anion-anion RDF is moved to longer *r*. Thus, the addition of the nucleobase at this higher concentration causes cations and anions to approach more closely, but causes some expansion in the arrangement of anions associated with an individual cation.

Looking at those uracil centred RDFs, it is clear that there are correlations to all three components in the solution: imidazolium cations, acetate anions and other uracil molecules. As might be expected, the strongest interactions appear with the anion – indeed, this interaction is even more pronounced for the 2:1 system with several clear oscillations (i.e. coordination shells) visible, perhaps as a result of increased structuring in the system (in line with the concomitant increase in viscosity at this ratio). Correlations between uracil and the cation and with other uracil molecules are also present, evidenced by significant peaks in the corresponding RDFs.

It is often more instructive to look at the three-dimensional distribution of species around a given reference molecule, than to rely on spherically-averaged RDFs. One such approach involves determining the positions of a given molecule type in some frame of reference defined using atomic sites on a central molecule in order to generate a system of axes. The positions of surrounding molecules may then be 'binned' on a three-dimensional grid according to their position from the central molecule, rather than just binning by distance as is the case for the RDF. The number of molecules found in a given 'bin' is indicative of the 'popularity' of that position and so, when averaged over all molecules and many frames, these 'spatial

probability densities' offer a snapshot of the preferred positions of one species relative to another. Plotting a surface which encompasses all positions above a certain threshold (a useful measure is typically the bulk number density of the molecule type) visually illustrates probable average positions of the molecules in 3D space. Such functions are shown in Figure 4 for the 2:1 mixture. Focusing first on the cation, we see the expected high density of anions aligned with the hydrogens of the imidazolium ring, and a slight reduction of anion along the side containing the ethyl group, owing to steric hindrance. Uracil molecules may also be found at relatively high density (three times bulk) around the cation, located above and below the plane of the ring with the molecule centres approximately 5 to 6 Å apart. These distances are somewhat long to be considered as a 'stacking' motif and, although the cation is occasionally approached by a uracil to form a parallel pair, the number and frequency of these contacts is negligibly small (see supplementary information, Figure SI.2). Around a central anion high probability regions for the cation and uracil molecules occupy the same positions around the anion suggesting direct competition between the two components for association through hydrogen-bonding with the anion carboxylate group. Around the uracil solute, prominent density equatorially arranged around the periphery of the molecule arises from correlations with the acetate anion as may be expected. However, some preferential positions for cation-uracil correlations do exist, and are mainly localised along the C=O bond vectors, suggesting some preferential interaction with hydrogen-bond donation from the cation to uracil carbonyl groups. There are also reasonably strong correlations between uracil molecules, as evidenced in the presence of relatively high

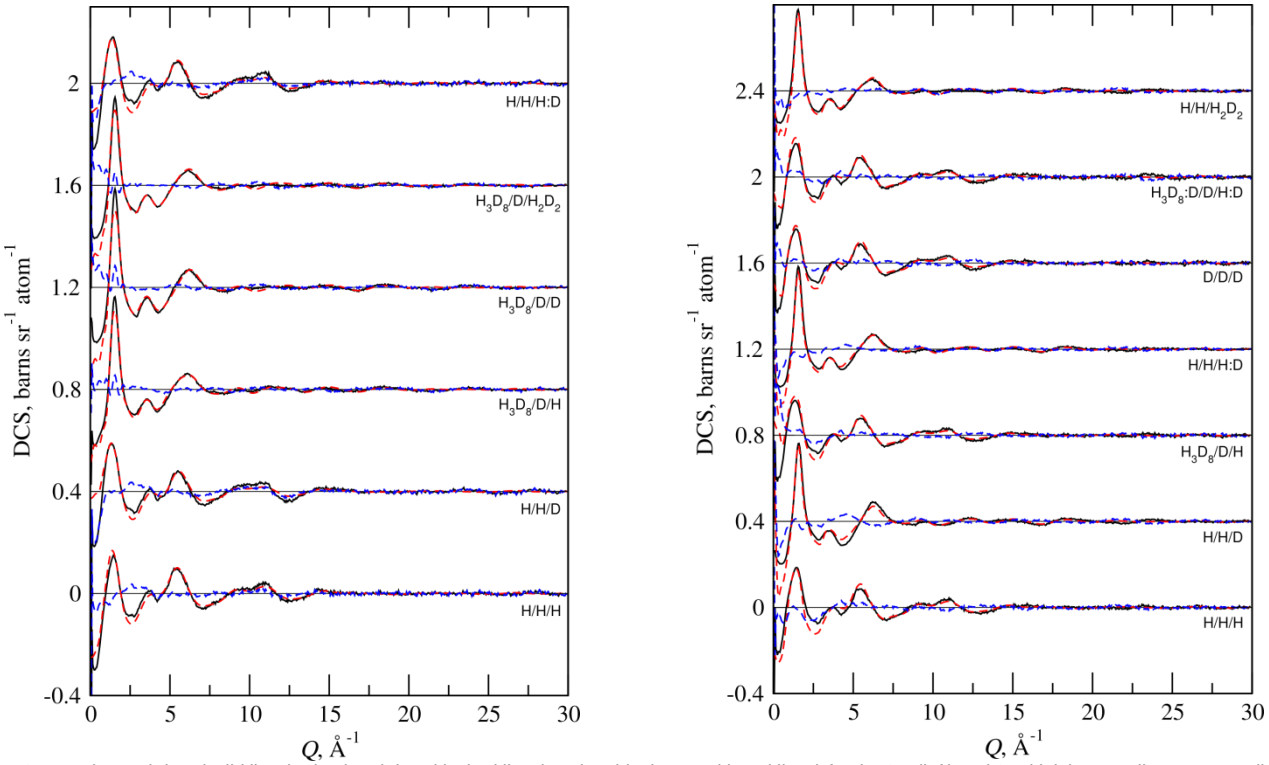

Figure 2. Experimental data (solid lines), simulated data (dashed lines) and residual errors (dotted lines) for the 2:1 (left) and 3:1 (right) IL:uracil systems studied.

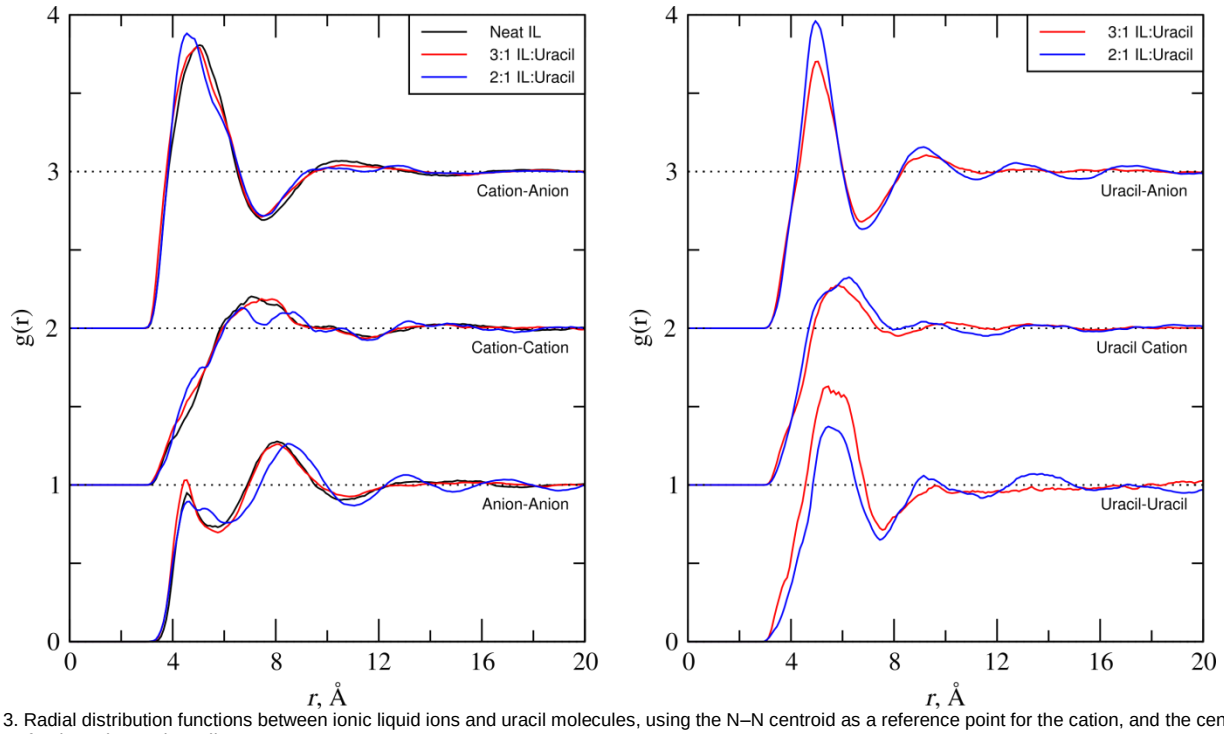

Figure 3. Radial distribution functions between ionic liquid ions and uracil molecules, using the N–N centroid as a reference point for the cation, and the centres of geometry for the anion and uracil.

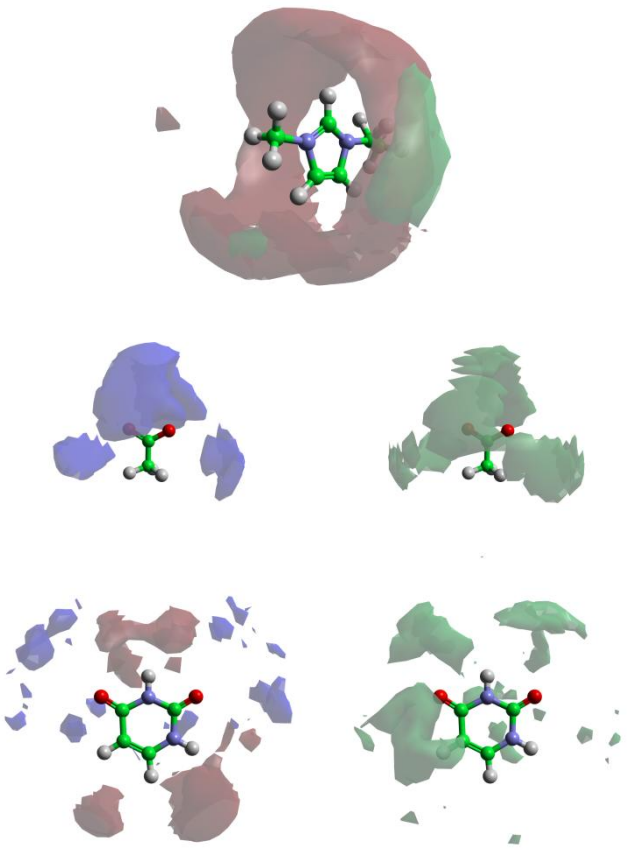

Figure 4. Spatial probability densities for cations (blue), anions (red) and uracil molecules (green) in the 2:1 system, showing preferred locations around a central cation and uracil. Surfaces shown are plotted at the following multiples of the bulk number density for each component: around the cation, 3 ρ for both anions and uracil; around the anion, 2.5 ρ for both cations and uracil, and; around uracil, 2 ρ for the cation, 3 ρ for the anion, and 2 ρ for uracil.

density lobes surrounding central molecule. The specific nature of these interactions will be probed in the following sections. For the 3:1 system the spatial distribution of species is similar (see Supplementary Information, Figure SI.3).

Cation-Anion Contacts

We begin by considering the general interaction pattern of the acetate anion with the 1-ethyl-3-ethylimidazolium cation. Looking at the partial RDFs between cation ring hydrogens and acetate oxygens (

Figure 5), we find strong correlations between the two sites. Considering all interactions less than 3.0 Å in length the $[EMIM]^+$ is involved in 2.63 H···O contacts in the pure liquid, reducing to 2.26 and 2.04 in the 3:1 and 2:1 mixtures respectively. This loss in the average number of cation-anion H···O contacts on the addition of uracil is consistent with the expected role of the anion in the solvation process, forming hydrogen bonds with the uracil molecules at the cost of those with the cation, and is evident in the partial RDFs as a decrease in intensity in the correlations.

An analysis of the contact patterns for these interactions is shown in Table 1 – for a given hydrogen site on the cation, the number of acetate oxygens within the cutoff distance is counted and grouped according to how the (potentially bidentate) acetate interacts with the site. The monodentate case (i.e. with a single hydrogen bond between the cation ring hydrogen and one oxygen of an acetate anion) predominates in both the pure ionic liquid and the mixtures, accounting for approximately two-thirds

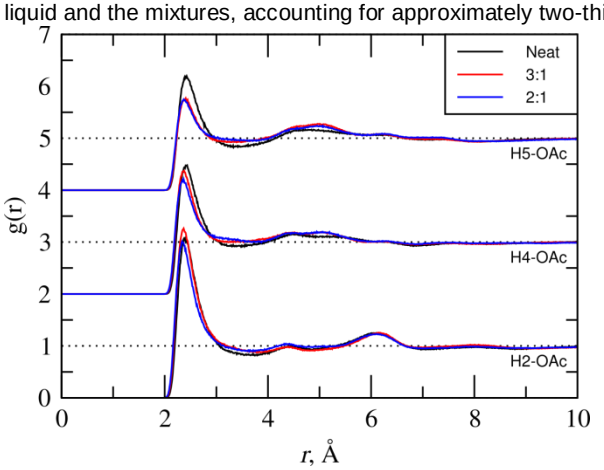

Figure 5. Partial RDFs between $[EMIM]^+$ ring hydrogens and acetate oxygen atoms. Curves for the neat IL system are derived from simulation of the data collected in the present study.

Table 1. Contact numbers per site between $[OAc]^-$ and $[EMIM]^+$ ring hydrogens (percentages of total interactions per site given in brackets).

System	Site	Total	Mono[a]	Bi[b]	Br[c]	Bif[d]	Other[e]
Neat[f]	H2	0.98	0.70 (72%)	0.28 (28%)	--	--	--
	H4	0.83	0.53 (63%)	0.17 (20%)	0.02 (3%)	0.06 (7%)	0.05 (6%)
	H5	0.75	0.46 (61%)	0.15 (20%)	0.02 (3%)	0.06 (8%)	0.06 (7%)
3:1	H2	0.94	0.67 (72%)	0.27 (28%)	--	--	--
	H4	0.73	0.50 (69%)	0.15 (21%)	0.03 (3%)	0.03 (4%)	0.03 (3%)
	H5	0.59	0.40 (68%)	0.11 (19%)	0.03 (4%)	0.03 (4%)	0.03 (4%)
2:1	H2	0.82	0.60 (73%)	0.22 (27%)	--	--	--
	H4	0.66	0.44 (67%)	0.13 (20%)	0.03 (4%)	0.03 (5%)	0.03 (4%)
	H5	0.56	0.37 (66%)	0.10 (18%)	0.03 (5%)	0.03 (6%)	0.03 (5%)

[a] Monodentate contacts where only one acetate oxygen is involved with the hydrogen. [b] Bidentate contacts where both oxygens are involved simultaneously with the same hydrogen (and thus is counted as two contacts). [c] Bridging interactions where both oxygens are involved simultaneously with different hydrogens. [d] Bifurcated contacts where one oxygen interacts simultaneously with two different hydrogens. [e] All other multiple-site contacts that cannot be easily quantified. [f] Calculated from EPSR simulations of the measured neat IL data in the present work, which employs different cutoff criteria than that presented in [5d].

of the interactions per ring hydrogen. Bidentate interactions account for approximately one quarter of interactions per site, with the small remainder consisting of bridging, bifurcated, and other multi-contact interactions (save for the H2 position where the monodentate and bidentate interactions account for all observed contacts).

Despite the decrease in the total number of contacts per site on the addition of uracil, the overall style of binding with the acetate anions remains largely unchanged. For instance, the H2 position always displays a relative ratio around 3:1 between monodentate and bidentate interactions with the acetate,

whereas it might have been expected that the number of 'wasteful' bidentate contacts would reduce as competition for the acetate anions increases. This may be taken as an indication of the strength of this particular geometric arrangement between cation and anion - i.e. the strength of binding between anions and uracil molecules is not enough to break this particular interionic interaction. On the other hand, if one considers the commonly-accepted interaction angle for a hydrogen bond (where X-H•••O > 150°) the bidentate geometry does permit additional hydrogen bonds with other molecules to be more easily formed than does the monodentate interaction.

Uracil-Anion Contacts

Figure 6 shows the partial RDFs between all uracil hydrogens and acetate oxygens, while **Table 2** provides details of the contact numbers per site. Using 'chemical intuition', the two amide hydrogens of uracil, HU1 and HU3, might expected to be the most strongly involved with the anion, and hence the dissolution process. Certainly, examination of the partial RDFs and contact numbers reveals that these two display significant short contacts with the acetate oxygens, but it is in fact HU6 which shows the most contacts. HU1 and HU3 are involved in around 1.27 contacts with O(Ac) between them in both the 2:1 and 3:1 systems, but HU6 is involved in 0.71 on its own. Conversely, the HU5 proton is involved in the fewest contacts (0.33). Looking at the distance-angle maps for the monodentate HU–$[OAc]^-$ contact, Figure 7, we see that those for HU1 and HU3 are the most well-defined and exhibit the shortest contact distances, strongly suggesting a hydrogen-bonding type interaction. HU6 also shows the same relatively strong indications of hydrogen bonding, albeit at a slightly longer average distance, while for HU5 the distribution is more disperse and at even longer distances.

These results are somewhat at odds with the proposal of reference 22, where only interaction with the amine-like HU1 and HU3 protons was suggested. We rationalise this by considering in more detail the local electronic environments present on the uracil. HU3 should, in principle, be strongly H-bonding, but its location in-between the two carbonyl groups at CU2 and CU4 leads to electronic repulsion of approaching acetate oxygens, since they themselves are negatively charged. HU1 is in a similar situation; however, with only one adjacent carbonyl (CU2), it is more accessible to the approaching $[OAc]^-$. This also goes some way towards explaining the relatively frequent occurrence of the bifurcated interaction between HU6 and HU1 (0.15 contacts per site). HU5, is adjacent to the O4 carbonyl and the HU6 proton of the C=C bond, and so is the least electronically suited interact with the acetate anion.

As with the cation, the predominant interaction geometry for the uracil protons with acetate oxygens is the monodentate form, accounting for between 30–80% of the interactions per site. Beyond this, except for HU3 where the only other observed contact is the bidentate mode, the bifurcated interaction is most commonly found, although the number of other, multi-centre contacts that are not so easily quantified is equally high.

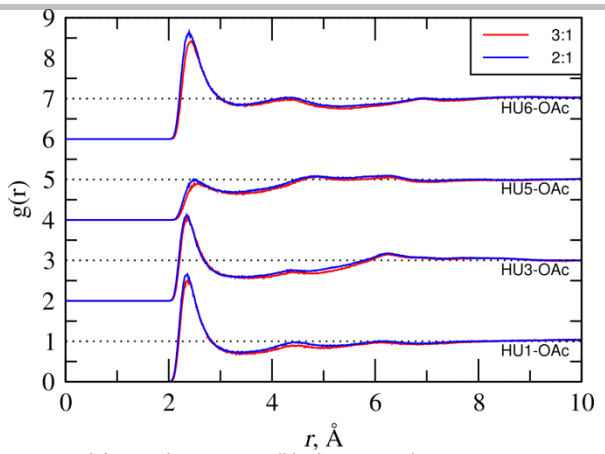

Figure 6. Partial RDFs between uracil hydrogens and acetate oxygen atoms.

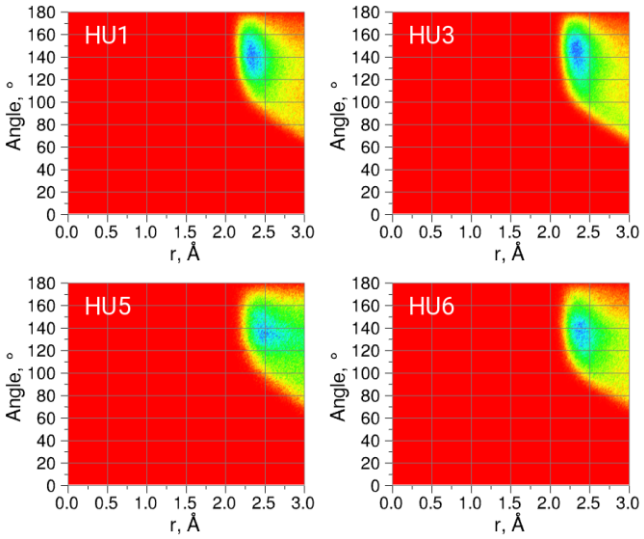

Figure 7. Distance-angle maps for monodentate contacts between HU and acetate oxygens.

Table 2. Contact numbers per site between $[OAc]^-$ and uracil hydrogens (percentages of total interactions per site given in brackets).

System	Site	Total	Mono[a]	Bi	Br	Bif	Other
3:1	HU1	0.71	0.31 (44%)	0.08 (11%)	0.02 (3%)	0.15 (21%)	0.15 (21%)
	HU3	0.56	0.44 (78%)	0.12 (22%)	--	--	--
	HU5	0.33	0.19 (58%)	0.03 (9%)	0.01 (4%)	0.06 (17%)	0.04 (11%)
	HU6	0.74	0.25 (34%)	0.06 (8%)	0.03 (5%)	0.21 (28%)	0.19 (25%)
2:1	HU1	0.69	0.30 (43%)	0.08 (11%)	0.02 (4%)	0.14 (21%)	0.14 (22%)
	HU3	0.54	0.41 (77%)	0.12 (23%)	--	--	--
	HU5	0.34	0.18 (53%)	0.03 (10%)	0.02 (5%)	0.06 (19%)	0.05 (14%)
	HU6	0.74	0.24 (32%)	0.06 (8%)	0.04 (5%)	0.20 (28%)	0.20 (27%)

[a] Designations for contact geometry are the same as in **Table 1**.

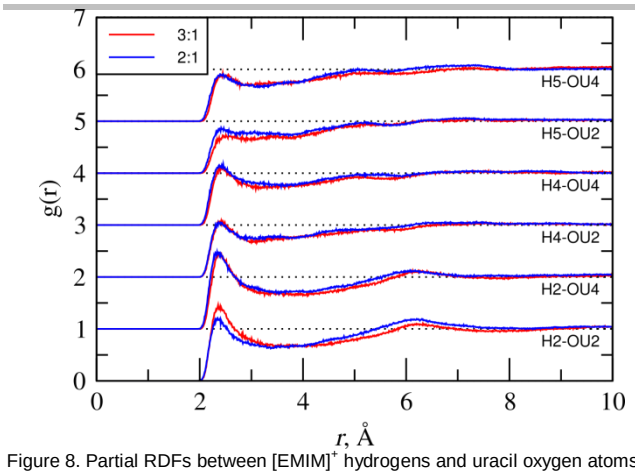

Figure 8. Partial RDFs between $[EMIM]^+$ hydrogens and uracil oxygen atoms.

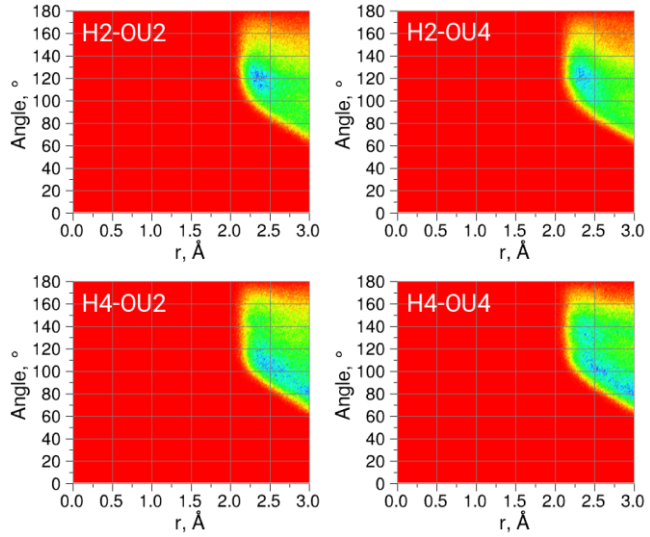

Figure 9. Distance-angle map for H2 and H4 contacts to uracil oxygens.

Uracil-Cation Contacts

One of the original postulates from the work of Araújo et al. was the existence of hydrogen bonds between the ring hydrogens of the cation (H2, H4, and H5) and the uracil carbonyl groups (OU2 and OU4).[21,22] The partial RDFs between these sites, Figure 8, certainly show some correlations, but with magnitudes that are considerably smaller than those of the corresponding acetate interactions. This is reflected in the contact numbers, Table 3, which are between 0.05–0.08 for the 3:1 system and 0.09–0.12 per site for the 2:1 system. While this slight increase in contact number with uracil concentration may be viewed in terms of the cation 'aiding' solvation as the number of available (and much stronger) acetate binding sites is reduced, one must also consider that cations are always associated with neighbouring anions. Figure 9 shows the distance-angle map for the H2···OU2(C) interaction, and reveals that most contacts occur with angles between 110 to 120°, and thus indicates that these interactions are not hydrogen bonding in nature. One might expect that interactions with the acidic hydrogen-bonding aromatic hydrogen sites of the cation would be observed at 'traditional' hydrogen bonding angles (i.e. greater than 150°) if the cation was independent of the anion, especially owing to the relative steric bulk of both the cation and uracil. The fact that this doesn't occur can be explained by the presence of anions around the HU3 and HU1 sites – the contact numbers between acetate oxygens and these sites (**Table 2**) are significant, and so may certainly be a factor in the close proximity of the cation H, which are also competing for interactions with the anion. Aside from these contacts, the primary solvation sphere of the uracil is relatively rich with the alkyl groups of the cation, as evidenced by the relevant partial RDFs (see Supporting Information, Figure SI.4).

Uracil-Uracil Contacts

Given the high concentrations of solutes in the systems studied here, it is reasonable to expect some favourable contacts between the solute molecules themselves to be observed. Table 4 lists the contact numbers between uracil hydrogens and oxygens, where we observe values of similar magnitude to those between cation hydrogens and the solute. Per uracil, the total number of solute-solute contacts is of the order of 0.65 in both concentrations studied. These addition contacts formed between uracil molecules may help to aid solubilsation in the ionic liquid by permitting localized pairing or clustering of solute molecules to occur, reducing the demand complete saturation of anions in the first coordination shell.

Table 3. Contact numbers per site between [EMIM]+ and uracil oxygens.

System	Site	OU2	OU4
3:1	H2	0.08	0.08
	H4	0.07	0.07
	H5	0.05	0.06
2:1	H2	0.10	0.12
	H4	0.10	0.11
	H5	0.09	0.09

Table 4. Contact numbers per site between uracil hydrogens and oxygens.

System	Site	OU2	OU4
3:1	HU1	0.08	0.09
	HU3	0.08	0.08
	HU5	0.08	0.07
	HU6	0.08	0.09
2:1	HU1	0.08	0.10
	HU3	0.10	0.10
	HU5	0.08	0.08
	HU6	0.10	0.10

Conclusions

A detailed analysis of the interactions present between cations, anions, and uracil molecules determined from neutron scattering on solutions of uracil in the IL, [EMIM][OAc], has been presented. We observe that hydrogen bonding contacts between cation ring-hydrogens and oxygen atoms of the acetate anion are reduced, relative to the pure ionic liquid, on the introduction of uracil, and decrease in proportion to the amount of uracil added, indicating that favourable contacts are formed between the anion (and/or the cation) and the nucleobase, providing the principal driver for dissolution.

Closer examination of the contacts between H and O sites on the uracil and the ionic liquid ions reveal that the reduction in cation-anion hydrogen bonding contacts is attributable to favorable interactions between acetate oxygens and uracil hydrogens, principally the HU6 and amine HU1 sites, which account for around 60% of this type of interaction (1.45 and 1.43 hydrogen bonds for the 3:1 and 2:1 systems respectively). The total number of acetate-uracil interactions remains similar for the 2:1 system (2.31 vs 2.34 contacts for 3:1) suggesting that even at the higher solute concentration there is still significant capacity for solvation, and is in line with reported solubilities of uracil in the IL up to 50 wt% (2:1 IL:uracil = 25 wt%).[21,22] Some uracil-uracil contacts are also observed and, while these interactions are not as significant as those formed between anion and uracil, permit uracil molecules to sit in close proximity to each other while dissolved. This has the effect of reducing the demand of a completely ionic-liquid-saturated primary coordination shell around the uracil, and permits high uracil:IL ratios to be achieved in practice.

Given the general reduction in the number of hydrogen bonding contacts between cation and acetate one may expect this to be manifest in an upfield shift of the relevant NMR proton signals on the cation, as was observed by Araújo et al. However, this does not necessarily mean that weaker hydrogen bonds are being formed with the uracil in consequence. Although we are able to count interactions between cation H atoms and uracil O atoms within typical (albeit weak) hydrogen bonding distances (rH•••O < 3.0 Å) the observed geometry of these contacts is atypical of hydrogen bonding interactions. Rather, the data suggests that upfield shifts in ^{1}H NMR signals due to H2, H4, and H5 protons reported in references 21 and 22 is predominantly due to loss of hydrogen bonds between cation and anion with the existence of cation-H···uracil-O close contacts being an effect arising from the proximity of acetate anions (which do bind relatively strongly to the nucleobase).

Experimental Section

Fully protiated [EMIM][OAc] (BASF) and uracil (>99%) were purchased from Sigma Aldrich. Deuteriated ionic liquids were synthesised following the methods detailed in references 5c and 5d (proton NMR spectra are show in Supporting Information, Figure SI.5). All ionic liquids were dried with stirring under high vacuum overnight. Fully deuteriated uracil (uracil-d_4) was synthesised by refluxing uracil-h_4 in acidified D_2O, taking advantage of the relatively high acidity of the protons.[24] Partially-deuteriated uracil (uracil-d_2) was synthesised by repeated washing of the fully-deuteriated product in H_2O before recrystallization. All were dried in a vacuum oven at 50°C overnight prior to use.

All neutron measurements were made on the Near and InterMediate Range Order Diffractometer (NIMROD) on Target Station 2 at ISIS, STFC Rutherford Appleton Laboratory, Harwell Campus. NIMROD offers access to total scattering data over a wide continuous Q range ($0.01 < Q < 50$ Å^{-1}) providing information on atomic correlations through to nanoscopic features entering into the small angle region. All samples were prepared and loaded into null-scattering $Ti_{0.676}Zr_{0.324}$ flat-plate cells inside an argon glove box in order to prevent the ingress of moisture into the systems. The cells have a nominal internal dimension of 40x38x1 mm WxHxD, giving an internal volume of 1.6 cc. The cells were sealed with a TiZr lid and PTFE O-ring, offering a vacuum-tight seal for the duration of the experiment. Samples were loaded onto a 15-position sample changer, and held at 25 °C using a Julabo FP50 circulating water bath.

Data processing of the raw neutron data was performed using the Gudrun package of Soper,[25] correcting for multiple-scattering and attenuation effects, removing inelasticity contributions from hydrogen, and placing the data on an absolute scale, normalised to a 3 mm vanadium plate standard sample. Analysis of the processed neutron data was made using the Empirical Potential Structure Refinement (EPSR) method of Soper.[26] Briefly, this approach involves the Monte Carlo simulation of a representative atomic system which is initially bounded by a supplied reference potential. In the present case, the reference potential (Lennard Jones parameters and atomic charges) for the ionic liquid and uracil were taken from the OPLS-AA forcefield[27] and the ionic liquid forcefield of Canongia Lopes and Padua.[28] Charges on the uracil were derived from fits to the electrostatic potential, calculated using GAMESS-US[29] at the optimised geometry calculated at the HF/6-31G(d) level. Once a Monte Carlo simulation of the system using these initial parameters has reached equilibrium an additional, empirical potential is introduced. This empirical potential is derived from the available experimental datasets, and is derived from the observed differences between calculated and experimental scattering functions, weighted by the scattering weights matrix for the individual partial structure factors. The application of this empirical potential encourages the Monte Carlo simulation towards closer agreement with the experimental data. Once suitable agreement is obtained, properties of interest may be extracted from the simulation in a manner analogous to those employed for standard Monte Carlo or molecular dynamics studies. Simulations of the pure IL system comprised 300 ion pairs (cubic box length 43.5399 Å), the 3:1 IL:uracil simulation 300 ion pairs and 100 uracil molecules (cubic box length of 44.8440 Å), and the 2:1 IL:uracil simulation 200 ion pairs and 100 uracil molecules (cubic box length of 39.9180 Å). All quantities were calculated using the 'dlputils' software.[30]

Acknowledgements

We thank the Science and Technology Facilities Council (STFC) for beam-time on NIMROD (ISIS experiment RB1320528) and the Department of Education and Learning in Northern Ireland (DEL) for a PhD studentships (to AHT).

Keywords: ionic liquids • neutron diffraction • liquids • uracil

[1] a) J. Estager, J. D. Holbrey, M. Swadzba-Kwasny *Chem. Soc. Rev.*, **2014**, *43*, 847-886; b) S. Tang, G. A. Baker, H. Zhao *Chem. Soc. Rev*. **2012**, *41*, 4030-4066; c) J. P. Hallett, T. Welton, *Chem. Rev*. **2011**, *111*, 3508-3576; d) J. E. Bara, D. E. Camper, D. L. Gin, R. D. Noble, *Acc. Chem. Res*. **2010**, *43*, 152-159; e) A. Pinkert, K. N. Marsh, S. Pang, M. P. Staiger, *Chem. Rev*. **2009**, *109*, 6712-6728; f) M. Armand, F. Endres, D. R. MacFarlane, H. Ohno, B. Scrosati, *Nat. Mater*. **2009**, *8*, 621-629.

[2] N. V. Plechkova, K. R. Seddon, *Chem. Soc. Rev*. **2008**, *37*, 123-150.

[3] C. Hardacre, J. D. Holbrey, M. Nieuwenhuyzen, T. G. A. Youngs, *Acc. Chem. Res*. **2007**, *40*, 1146-1155.

[4] M. Y. Lui, L. Crowhurst, J. P. Hallett, P. A. Hunt, H. Niedermeyer, T. Welton, *Chem. Sci*. **2011**, *2*, 1491-1496.

[5] a) S. E. Norman, A. H. Turner, T. G. A. Youngs, *RSC Adv*. **2015**, *5*, 67220-67226; b) H. Cruz, M. Fanselow, J. D. Holbrey, K. R. Seddon, *Chem. Commun.* **2012**, *48*, 5620-5622; c) T. G. A. Youngs, J. D. Holbrey, C. L. Mullan, S. E. Norman, M. C. Lagunas, C. D'Agostino, M. D. Mantle, L. F. Gladden, D. T. Bowron, C. Hardacre., *Chem. Sci.* **2011**, *2*, 1594-1605; d) D. T. Bowron, C. D'Agostino, L. F. Gladden, C. Hardacre, J. D. Holbrey, M. C. Lagunas, J. McGregor, M. D. Mantle, C. L. Mullan, T. G. A. Youngs, *J. Phys. Chem. B* **2010**, *114*, 7760-7768; e) L. Vanoye, M. Fanselow, J. D. Holbrey, M. P. Atkins, K. R. Seddon, *Green Chem*. **2009**, *11*, 390-396; f) T. G. A. Youngs, C. Hardacre, J. D. Holbrey, *J. Phys. Chem., B* **2007**, *111*, 13765-13774; g) T. G. A. Youngs, J. D. Holbrey, M. Deetlefs, M. Nieuwenhuyzen, M. F. Costa Gomes, C. Hardacre, *ChemPhysChem.* **2006**, *7*, 2279-2281.

[6] R. P. Swatloski, S. K. Spear, J. D. Holbrey, R. D. Rogers, *J. Am. Chem. Soc.* **2002**, *124*, 4974-4975.

[7] Y. Fukaya, K. Hayashi, M. Wada, H. Ohno, *Green Chem*. **2008**, *10*, 44-46.

[8] R. Rinaldi, *Chem. Commun*. **2011**, *47*, 511-513.

[9] C. Mao, Z. Wang, Z. Wang, P. Ji, J.-P. Cheng, *J. Am. Chem. Soc*. **2016**, *138*, 5523–5526.

[10] O. A. El Seoud, A. Koschella, L. C. Fidale, S. Dorn, T. Heinze, *Biomacromol.* **2007**, *8*, 2629-2647.

[11] J.-H. Wang, D.-H. Cheng, X.-W. Chen, Z. Du, Z.-L. Fang, *Anal. Chem*. **2007**, *79*, 620-625.

[12] J.-C. Plaquevent, J. Levillain, F. Guillen, C. Malhiac, A.-C. Gaumont, *Chem. Rev*. **2008**, *108*, 5035-5060.

[13] a) M. C. Uzagare, Y. S. Sanghvi, M. M. Salunkhe, *Green Chem.* **2003**, *5*, 370-372; b) V. Kumar, V. S. Parmar, S. V. Malhotra, *Tetrahedron Letts*. **2007**, *48*, 809-812; c) C. Hardacre, H. Haifeng; S. L. James, M. E. Migaud, S. E. Norman, W. R. Pitner, *Chem. Commun*. **2011**, *47*, 5846-5848.

[14] a) Y. Zhao, J. Wang, H. Wang, Z. Li, X. Liu, S. Zhang, *J. Phys. Chem. B* **2015**, *119*, 6686-6695; b) V. Lesch, A. Heuer, C. Holm, J. Smiatek, *Phys. Chem. Chem. Phys*. **2015**, *17*, 8480-8490; c) B. D. Rabideau, A. Agarwal, A. E. Ismail, *J. Phys. Chem. B* **2014**, *118*, 1621-1629; d) H. Liu, G. Cheng, M. Kent, V. Stavila, B. A. Simmons, K. L. Sale, S. Singh, *J. Phys. Chem. B* **2012**, *116*, 8131-8138; e) H. Liu, K. L. Sale, B. A. Simmons, S. Singh, *J. Phys. Chem. B* **2011**, *115*, 10251-10258.

[15] a) M. E. Ries, A. Radhi, A. S. Keating, O. Parker, T. Budtova, *Biomacromol*. **2014**, *15*, 609-617; b) J. Zhang, H. Zhang, J. Wu, J. Zhang, J. He, J. Xiang, *Phys. Chem. Chem. Phys*. **2010**, *12*, 1941-1947.

[16] a) H. Wang, G. Gurau, S. V. Pingali, H. M. O'Neill, B. R. Evans, V. S. Urban, W. T. Heller, R. D. Rogers, *ACS Sus. Chem*. **2014**, *2*, 1264-1269; b) G. Cheng, M. S. Kent, L. He, P. Varanasi, D. Dibble, R. Arora, K. Deng, K. Hong, Y. B. Melnichenko, B. A. Simmons, S. Singh, *Langmuir* **2012**, *28*, 11850-11857.

[17] a) L. Wu; S.-H. Lee; T. Endo, *Bioresource Technology,* **2013**, *140*, 90-96. b) F. Xie; B. M. Flanagan; M. Li; P Sangwan; R. W. Truss; P. J. Halley; E. V. Strounina; A. K. Whittaker; M. J. Gidley; K. M. Dean, *Carbohydrate Polymers* **2014**, *111*, 841-848

[18] a) H. –C. Chang; R. –L. Zhang; D. –T. Hsu, *Phys. Chem. Chem Phys.* **2015**, *17*, 27573-27578; b) J. Kiefer; K. Obert; A. Boesmann; T. Seeger; P. Wasserscheid; A. Leipertz, *ChemPhysChem* **2008**, *9*, 1317-1322.

[19] a) W. M. Reichert, J. D. Holbrey, R. P. Swatlowski, K. E. Gutowski, A. E. Visser, M. Nieuwenhuyzen, K. R. Seddon and R. D. Rogers, *Cryst. Growth and Design* **2007**, *7*, 1106-1114; b) P. Kölle and R. Dronskowski, *Inorg. Chem*. **2004**, *43*, 2803–2809.

[20] a) J. D. Holbrey, W. M. Reichert, I. Tkatchenko, E. Bouajila, O. Walter, I. Tommasi and R. D. Rogers, *Chem. Commun.* **2003**, 28-29; b) J. A. Stewart, R. Drexel, B. Arstad, E. Reubsaet, B. M. Weckhuysen and P. C. A. Bruijnincx, *Green Chem*. **2016**, *18*, 1605-1618.

[21] J. M. Araújo, R. Ferreira, I. M. Marrucho, L. P. N. Rebelo, *J. Phys. Chem. B* **2011**, *115*, 10739-10749.

[22] J. M. Araújo, A. B. Pereiro, J. N. Canongia-Lopes, L. P. Rebelo, I. M. Marrucho, *J. Phys. Chem. B* **2013**, *117*, 4109-4120.

[23] H. Tateishi-Karimata and N. Sugimoto, *Nucl. Acids Res.* **2014**, 1.

[24] M. A. Kurinovich, K. J. Lee, *J. Am. Soc. Mass Spec.* **2002**, *13*, 985-995.

[25] A. K. Soper, S. W. Howells and A. C. Hannon, "*ATLAS-Analysis of Time-of-Flight Diffraction Data from Liquid and Amorphous Samples*", Report RAL-89-046; Rutherford Appleton Laboratory, 1989.

[26] A. K. Soper, *Chem. Phys*. **1996**, *202*, 295-306; A. K. Soper, *Chem. Phys*. **2000**, *258*, 121-137; A. K. Soper, *Mol. Phys.* **2001**, *99*, 1503-1516.

[27] W. L. Jorgensen and J. Tirado-Rives, *J. Am. Chem. Soc.* **1996**, *110*, 1657-1662.

[28] a) J. N. Canongia Lopes, A. A. H. Padua, *J. Phys. Chem. B* **2006**, *110*, 19586-19592; b) J. N. Canongia Lopes, J. Deschamps, A. A. H. Padua, *J. Phys. Chem. B* **2004**, *108*, 2038-2047; c) J. N. Canongia Lopes, A. A. H. Padua, J. Deschamps, *J. Phys. Chem. B* **2004**, *108*, 11250-11250.

[29] a) M. W. Schmidt, K. K. Baldridge, J. A. Boatz, S. T. Elbert, M. S. Gordon, J. H. Jensen, S. Koseki, N. Matsunaga, K. A. Nguyen, S. Su, T. L. Windus, M. Dupuis, J. A. Montgomery, *J. Comput. Chem.* **1993**, *14*, 1347-1363; M. S. Gordon, M. W. Schmidt, C. E. Dykstra, G. Frenking, K. S. Kim, and G. E. Scuseria (ed.), Theory and Applications of Computational Chemistry: the first forty years Advances in electronic structure theory: GAMESS a decade later Elsevier (Amsterdam), 2005, p. 1167.

[30] 'dlputils' software, https://www.projectaten.com/dlputils, retrieved June 2015.